remote sensing

MDPI

Article

Satellite-Derived Lagrangian Transport Pathways in the Labrador Sea

Renato M. Castelao [1,*], Hilde Oliver [2] and Patricia M. Medeiros [1]

[1] Department of Marine Sciences, University of Georgia, Athens, GA 30602, USA
[2] Applied Ocean Physics and Engineering Department, Woods Hole Oceanographic Institution, Woods Hole, MA 02543, USA
* Correspondence: castelao@uga.edu

Abstract: The offshore transport of Greenland coastal waters influenced by freshwater input from ice sheet melting during summer plays an important role in ocean circulation and biological processes in the Labrador Sea. Many previous studies over the last decade have investigated shelfbreak transport processes in the region, primarily using ocean model simulations. Here, we use 27 years of surface geostrophic velocity observations from satellite altimetry, modified to include Ekman dynamics based on atmospheric reanalysis, and virtual particle releases to investigate seasonal and interannual variability in transport of coastal water in the Labrador Sea. Two sets of tracking experiments were pursued, one using geostrophic velocities only, and another using total velocities including the wind effect. Our analysis revealed substantial seasonal variability, even when only geostrophic velocities were considered. Water from coastal southwest Greenland is generally transported northward into Baffin Bay, although westward transport off the west Greenland shelf increases in fall and winter due to winds. Westward offshore transport is increased for water from southeast Greenland so that, in some years, water originating near the east Greenland coast during summer can be transported into the central Labrador Sea and the convection region. When wind forcing is considered, long-term trends suggest decreasing transport of Greenland coastal water during the melting season toward Baffin Bay, and increasing transport into the interior of the Labrador Sea for water originating from southeast Greenland during summer, where it could potentially influence water column stability. Future studies using higher-resolution velocity observations are needed to capture the role of submesoscale variability in transport pathways in the Labrador Sea.

Keywords: Labrador Sea; Lagrangian trajectories; transport pathways; Greenland

Citation: Castelao, R.M.; Oliver, H.; Medeiros, P.M. Satellite-Derived Lagrangian Transport Pathways in the Labrador Sea. *Remote Sens.* **2023**, *15*, 5545. https://doi.org/10.3390/rs15235545

Academic Editor: Mark Bourassa

Received: 2 October 2023
Revised: 21 November 2023
Accepted: 21 November 2023
Published: 28 November 2023

1. Introduction

The Labrador Sea off southwest Greenland is known to be a site of intermediate water formation [1–3]. It also hosts some of the most productive waters of the subarctic North Atlantic Ocean, with highly productive phytoplankton blooms during spring and summer [4,5]. The Labrador Sea is influenced by the seasonal input of Arctic-sourced freshwater that is transported southward along east Greenland [6], both by coastal currents and farther offshore by the slope current [7]. The region has been under the influence of substantial changes over the last few decades, as melting from the Greenland ice sheet has accelerated [8–12]. Increased freshwater fluxes from the Greenland ice sheet can play an important role in the freshwater budget of the subarctic Atlantic [10], with model simulations revealing its contribution to a gradual freshening near the surface in the Labrador Sea [13]. This has received great interest from the scientific community due to its potential for weakening the intensity of winter convection due to increased water column stability [14,15]. Changes in meltwater distribution in the Labrador Sea may also have large implications for the marine ecosystem primary productivity by changing nutrient availability and mixed-layer depths [16–20]. The arrival of glacial meltwater in the

northern Labrador Sea has been shown to often coincide with the development of summer phytoplankton blooms [5].

The potential for coastal water off southern Greenland to influence physical and biogeochemical processes in the Labrador Sea will depend on the preferred transport pathways in the region, as the coastal water may be transported to different regions during different times of the year. The general circulation in the Labrador Sea is cyclonic, with the northward-flowing West Greenland Current (WGC) off southwest Greenland and the southward-flowing Labrador Current off Eastern Canada. The mean currents off west Greenland generally veer westward, connecting the two current systems (Figure 1a; see Figure 1 in Pickart et al. [21] for a schematic of the circulation). Currents off southwest Greenland have been shown to be particularly unstable, being a source of eddies in the region [22,23].

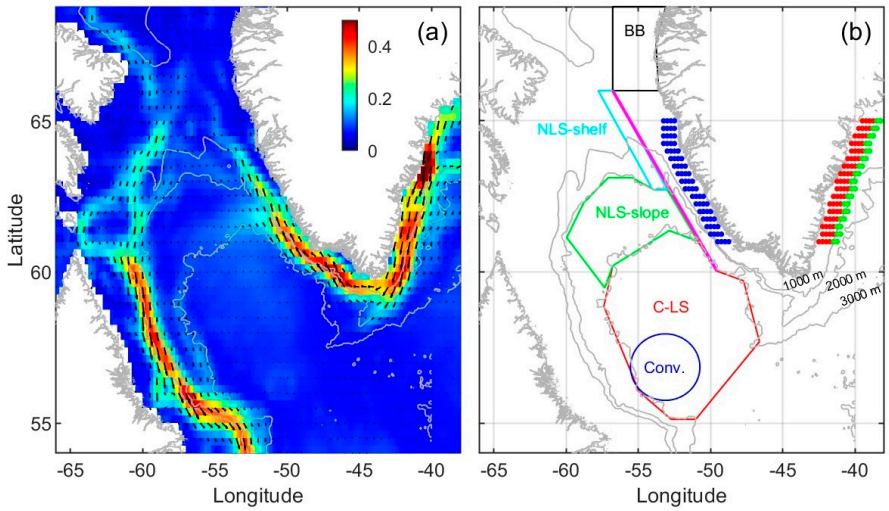

Figure 1. (**a**) Long-term average (1993−2019) of total surface velocities from OSCAR. Colors show average velocity magnitude (ms^{-1}). (**b**) Small dots near the coast reveal location of virtual drifter releases off southwest Greenland (blue) and off southeast Greenland, near the coast (red) and farther offshore (green). Polygons in the Labrador Sea indicate the areas used for identifying drifter transport: Baffin Bay (BB), northern Labrador Sea (NLS) shelf and slope, central Labrador Sea (C-LS), and convection region (Conv.). The magenta line parallel to the southwest Greenland coast was used to identify the latitude where drifters moved westward. The 1000, 2000 and 3000 m isobaths are shown in gray.

Many studies over the last decade have focused on investigating transport processes in the Labrador Sea [24–28], several of them with a particular focus on understanding the transport pathways of meltwater originating from the Greenland ice sheet [13,29–31]. These studies generally showed that the Labrador Sea can be influenced both by local inputs of meltwater from the Greenland ice sheet off southwest Greenland but also by inputs off southeast Greenland as the meltwater is transported toward the Labrador Sea in the East Greenland Current. Wind forcing off southwest Greenland has also been shown to strongly influence the transport of coastal water in the Labrador Sea [27,29,31]. The majority of these studies relied on results from ocean models to identify transport. Here, we used observations of surface geostrophic velocities from satellite altimetry, modified to include Ekman dynamics based on ocean vector winds from reanalysis (Ocean Surface Current Analyses Real-time—OSCAR; [32]) and virtual drifters [33] to investigate spatial and temporal variability in the transport of coastal water from southwest and southeast Greenland in the Labrador Sea. OSCAR surface velocities are available since 1993, which allowed for transport pathways of coastal water associated with large-scale or mesoscale surface dynamics to be characterized on seasonal and interannual scales. We investigated transport pathways throughout the entire year but focused on interannual variability

during summer, when coastal waters off south Greenland are under the largest influence of meltwater from the Greenland ice sheet [34].

2. Methods

Daily surface currents on a 0.25° grid were obtained from Ocean Surface Current Analyses Real time (OSCAR) version 2.0. OSCAR surface currents are calculated from satellite observations using a simplified physical model of an upper-ocean turbulent mixed layer and include a geostrophic term, a thermal wind adjustment, and a wind-driven term [32]. The geostrophic component of the velocity is computed using satellite altimetry, specifically the delayed-time absolute dynamic topography global gridded product distributed by the Copernicus Marine Environment Monitoring Service (CMEES; https://doi.org/10.48670/moi-00148). Total velocities are calculated, including the thermal wind adjustment term and the effects of Ekman dynamics, using ERA5 10 m reanalysis vector winds produced by the European Centre for Medium-Range Weather Forecasts (ECMWF; [35]). Currents are provided as an averaged value over the top 30 m of the solution ([32]; Figure 1a).

To characterize the circulation in the Labrador Sea, we pursued Lagrangian tracking experiments of virtual passive particles [36] using Parcels ([33]; https://oceanparcels.org, accessed on 20 November 2022). Particles were released every 5 days from January 1993 to December 2019. For each seeding event (i.e., every 5 days), 170 virtual particles were released, 68 off coastal southwest Greenland, 68 off coastal southeast Greenland, and 34 farther offshore off southeast Greenland (Figure 1b). A total of 335,070 particles were released during the 27 years considered here. The spacing between particles at the time of release was 0.25° to approximately match the grid spacing of OSCAR. Particles were tracked forward in time using the fourth-order Runge–Kutta scheme [36] for at least 8 months, by which time they generally had either left the domain or become grounded (i.e., reached a region where the velocity field is not defined, such as the land–ocean interface). A diffusion term was not considered. Two sets of tracking experiments were pursued, one using geostrophic velocities only and the other using total velocities, which include the wind-driven term [32]. Comparing the results from the two sets of experiments allowed for the influence of wind forcing to be inferred. We note that a recent comparison between simulated particle trajectories using satellite altimetry and the trajectories of 34 Surface Velocity Program (SVP) surface drifters deployed in the region revealed that altimetry-derived surface currents are capable of recovering the spatial structure of the flow field over the shelf off south Greenland, capturing the nature of the flow, as observed from the surface drifters [37].

Heat maps of particle distributions from the three different sources (coastal southwest, coastal southeast, and offshore southeast Greenland; Figure 1b) were built on a monthly time scale using a 0.5° × 0.5° grid. Our analyses revealed that many of the particles released off southeast Greenland, especially those released near the coast, ended up being transported toward land and, therefore, became stuck shortly after release. Thus, these particles ended up never being transported to the west of the southern tip of Greenland into the Labrador Sea. To minimize this effect, only particles that were transported to the west of 45°W at some point in their trajectories were considered. After discarding particles that became grounded off southeast Greenland, to the east of 45°W, we tracked all particles that were released in a given month of a given year, and we identified the fraction of those particles that passed through each 0.5° × 0.5° bin. That ratio was then multiplied by 100 to yield a percentage. Repeating the analysis for all months over the 27 years considered here yielded 324 maps of particle distribution for each of the 3 sources. Empirical orthogonal function (EOF) decompositions were pursued to identify the dominant modes of variability in particle distribution. Increases in the number of particles that were released in a given month at a certain location indicate an increase in transport toward that location.

Previous studies have shown that water off southwest Greenland in the Western Greenland Current is often transported westward in a cyclonic fashion, approximately following

the isobaths, circumnavigating the Labrador Sea [38]. The latitude of the westward offshore transport varies seasonally [39]. To quantify this, we identified the latitudes at which particles from the 3 different sources released each month crossed the magenta line (parallel to the coastline) in Figure 1b. For each seeding event (i.e., every 5 days), we also quantified the fraction of particles from each of the 3 sources that reached different subregions in the Labrador Sea. Once again, particles that became grounded off southeast Greenland, to the east of 45°W, were not included in the analysis. The different subregions in the Labrador Sea considered here are shown in Figure 1b and included the central Labrador Sea (delineated by the 3000 m isobath), the area in the interior of the basin characterized by winter convection [21], and the northern Labrador Sea shelf and slope (somewhat arbitrarily divided by the 2000 m isobath). These regions are located away from the coastal zone, capturing particles that are transported westward into the Labrador Sea to the south of 66°N. The last region focused on the coastal area off west Greenland, capturing particles that did not move westward to the south of 66°N. This encompasses both particles that were transported to southern Baffin Bay and particles that became grounded off southwest Greenland. Our analyses revealed that several particles (both those released off southwest and off southeast Greenland) were transported toward shore off southwest Greenland, which resulted in them becoming grounded. Given that those particles were generally being transported northward in the WGC while they moved onshore, they were grouped here with the particles that were transported toward southern Baffin Bay (i.e., forming a group of particles that were not transported westward to the south of 66°N). Since particles may be transported into more than one subregion; the sums of the fraction of particles from each source that reached the 5 subregions generally exceeded 100%. Lastly, in addition to looking at seasonal patterns in the transport of virtual particles toward those 5 subregions, we also investigated variability between the years for particles released between mid-July and late September. This is because this is the time of the year when clear signatures of meltwater input from the Greenland ice sheet are found off south Greenland [34]. We refer to this period here as the melting season.

Winds were obtained from the Cross-Calibrated Multi-Platform (CCMP) version 3.0 product, which is a combination of ocean surface wind retrievals from multiple types of satellite microwave sensors and a background field (ERA5) from reanalysis [40]. The product is available on a 0.25° grid with a temporal resolution of 6 h. Cumulative alongshelf wind stress [41] averaged within 100 km from the coast off southwest Greenland between 61 and 65°N was computed to characterize average wind conditions in the region (Figure 2). Decreases or increases in cumulative wind stress off southwest Greenland indicate predominantly upwelling- or downwelling-favorable winds, respectively [29,31].

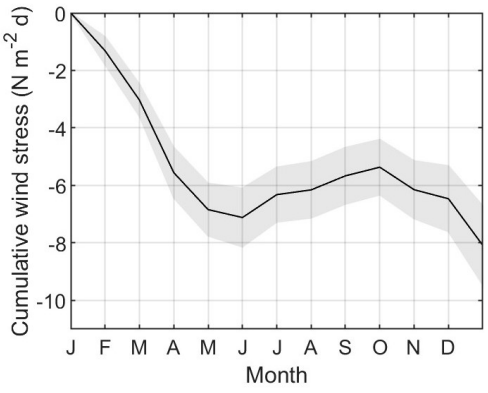

Figure 2. Cumulative alongshore wind stress off southwest Greenland from 1993 to 2018, averaged within 100 km from shore. The black line shows the mean value, while the shaded gray area indicates ±1 standard error of the mean. Decreases in cumulative alongshelf wind stress indicate predominant upwelling favorable winds, while increases indicate downwelling favorable winds.

3. Results

Average winds off coastal southwest Greenland are upwelling-favorable from late fall to early spring and weakly downwelling-favorable during summer (Figure 2). Substantial variability is observed during summer [29], however, with predominantly upwelling-favorable winds being observed in 1 out of every 3 years [31]. Particles released in coastal waters off southwest and southeast Greenland (Figure 1b) were tracked to identify preferred transport pathways between the coastal ocean and other regions of the Labrador Sea and southern Baffin Bay. Examples of trajectories for particles released on 27 August 2008 are shown in Figure 3, and they illustrate some of the main transport pathways in the basin. While, on average, coastal winds during summer off southwest Greenland are predominantly to the northwest (Figure 2), they were predominantly to the southeast during summer 2008 [29,31]. In all cases, most particles were transported around the Labrador Sea cyclonically, roughly following isobaths (Figure 3). When considering only geostrophic velocities, a substantial fraction of particles released off southwest Greenland were transported northward into Baffin Bay (Figure 3a), while particles released off southeast Greenland were mostly transported westward after reaching southwest Greenland (Figure 3b). When total velocities including the wind-driven term were used, an increased tendency for westward transport of particles was observed. Fewer particles released off southwest Greenland were transported toward the northern sector of the domain (Figure 3c), while several of those released off southeast Greenland were transported westward across isobaths into the central Labrador Sea (Figure 3d).

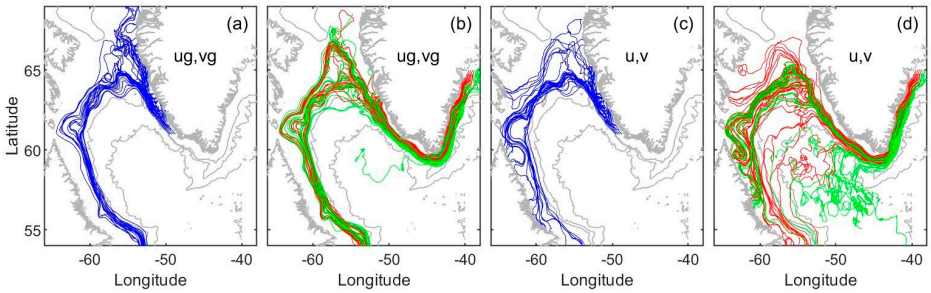

Figure 3. Examples of virtual drifter trajectories released on 27 August 2008 off (**a**,**c**) southwest (blue) and (**b**,**d**) southeast Greenland (coastal in red, offshore in green) using (**a**,**b**) only the geostrophic component of the flow (ug, vg) or (**c**,**d**) total velocities including the wind-driven term (u, v). The 1000, 2000 and 3000 m isobaths are shown in gray.

3.1. Dominant Modes of Variability in Transport Pathways

The trajectories of all particles released at a 5-day interval over 27 years were used to build heat maps of particle distribution, i.e., to identify how frequently particles from a given source released in a particular month were observed at each location in a $0.5^\circ \times 0.5^\circ$ grid. Empirical orthogonal decompositions (EOF) were then used to identify the dominant modes of variability in those distributions. When only geostrophic velocities are considered, particles released from southwest Greenland are most frequently observed near their release location and then in a thin (~60 km wide) band extending around the basin close to the 1000 m isobath (Figure 4a). The first EOF mode (Figure 4b) captures an increase in the frequency of particles along that pathway that were released during fall peaking in October, and a decrease in spring (Figure 4e), although there is substantial interannual variability, with larger positive peaks in the first half of the time series (Figure 4d). The second EOF mode captures a slight tendency for particles released in late summer/early fall to be transported northward toward Baffin Bay and westward for those released in winter (Figure 4c,g). When total velocities, which include the wind-driven term, are considered, the average distribution of particles released off southwest Greenland remains similar (Figure 5a) to when only the geostrophic component was used (Figure 4a). The strongest seasonal change in the frequency of observing particles captured by EOF 1 is slightly

shifted southward, occurring primarily between the 1000 and 2000 m isobaths (area in red in Figure 5b). Peak frequency along that pathway occurs for particles released in winter, while for particles released during summer, the frequency between the 1000 and 2000 m isobaths decreases (Figure 5d,e). For particles released during late winter and spring, EOF 2 captured a slight shift in the trajectories toward the 2000 m isobath (Figure 5c,f,g), while for those released during fall, the increase in the frequency of particles was observed in waters shallower than the 1000 m isobath (blue areas in Figure 5c).

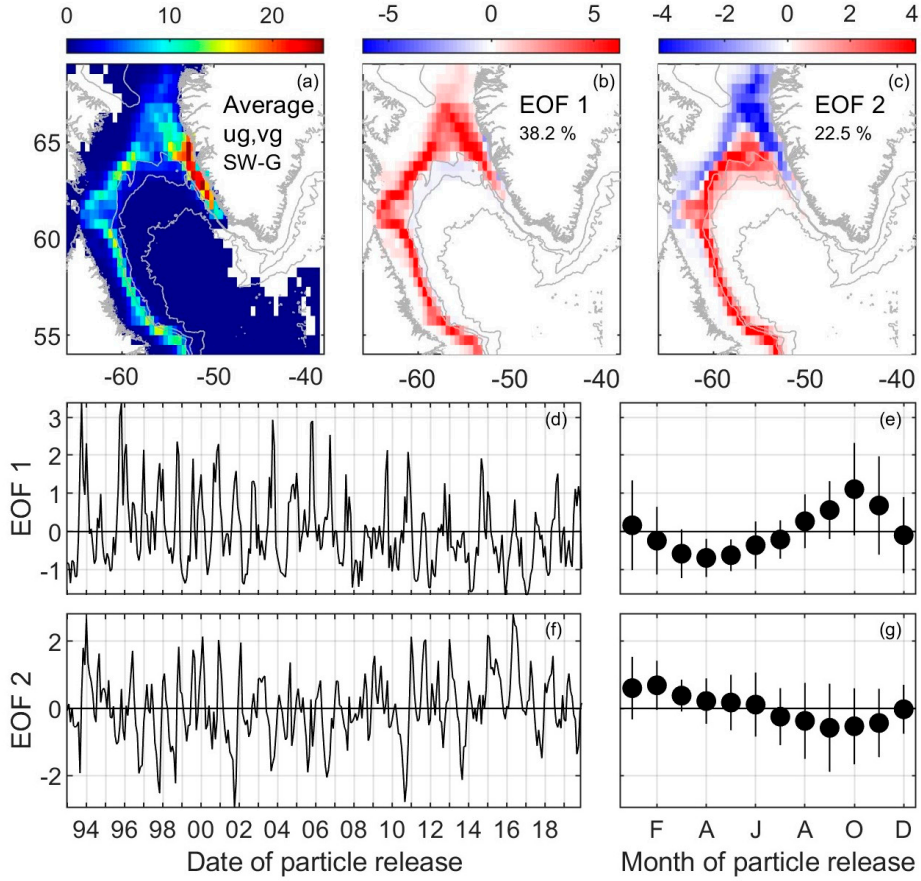

Figure 4. Heat maps showing distribution of particles released off southwest Greenland (SW−G) using only the geostrophic component of the velocity (ug, vg). (**a**) Average (%), (**b**) EOF 1 and (**c**) EOF 2, and amplitude time series for (**d**) EOF 1 and (**f**) EOF 2. Monthly averages of the amplitude time series for (**e**) EOF 1 and (**g**) EOF 2 are also shown. Amplitude time series indicate timing of particle release. Fraction of variance explained by EOFs 1 and 2 are shown in panels (**b**,**c**).

For particles released in coastal waters off southeast Greenland (red dots in Figure 1b), the average distribution of the frequency of observing particles at a given location when only geostrophic velocities are considered is consistent with transport in the Eastern and Western Greenland Currents (Figure 6a; [38]). Large values are observed in coastal waters off southeast and southwest Greenland and also around the 1000 m isobath circumnavigating the Labrador Sea. Once again, a large seasonal change in the distribution of particles is captured by EOF 1 just north and west of the 1000 m isobath (Figure 6b), representing an increase in the frequency for particles released during August to October and a decrease for those released during winter (Figure 6d,e). EOF1 values are slightly negative between the 2000 and 3000 m isobath, indicating increased transport in that region during winter (Figure 6e). Positive EOF 2 values are increased between the 1000 and 2000 m isobaths, with smaller negative values extending toward Baffin Bay (Figure 6c). The mode is not characterized by clear seasonal variability (Figure 6g) but instead by large pulses in different

years (Figure 6f). When total velocities are considered (Figure 7a), the average distribution of particles released off coastal southeast Greenland in the Labrador Sea is similar to when only the geostrophic component is used, although the intensification around the 1000 m isobath is somewhat reduced (compare Figure 7a with Figure 6a). The first EOF mode captures the westward transport of particles released during summer (Figure 7e) to the north and west of the 1000 m isobath (areas in red Figure 7b). It also captures variability in the distribution of particles released in winter (Figure 7e) off coastal southeast Greenland that extends over a much larger area of the Labrador Sea, including into the interior of the basin (areas in blue in Figure 7b). EOF 2 is primarily characterized by large positive values between the 1000 and 2000 m isobaths (Figure 7c). Monthly averages of the amplitude time series for EOF 2 are generally not different from zero (Figure 7g), but several large events are observed throughout the years (Figure 7f). EOFs of the distribution of particles released farther offshore off southeast Greenland (particles in green in Figure 1b) reveal a picture consistent with that described for particles released near the coast (Figures 6 and 7) but with increased EOF values extending farther into the interior of the basin.

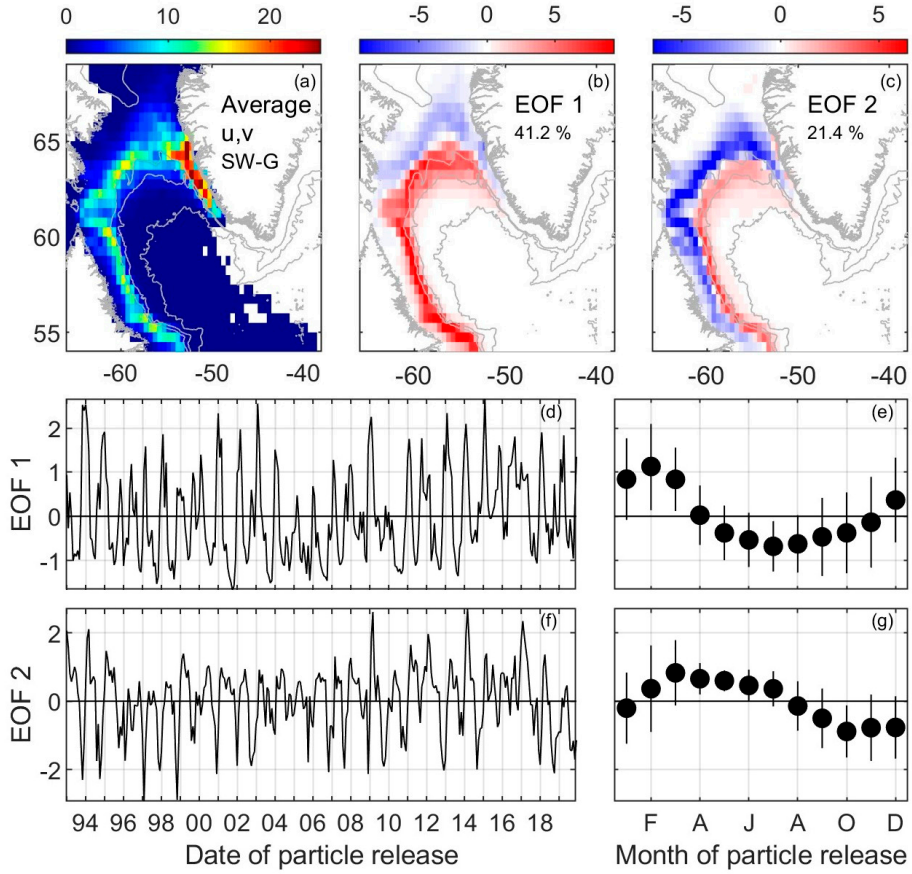

Figure 5. Heat maps showing distribution of particles released off southwest Greenland (SW−G) using total velocities including the wind effect (u, v). (**a**) Average (%), (**b**) EOF 1 and (**c**) EOF 2, and amplitude time series for (**d**) EOF 1 and (**f**) EOF 2. Monthly averages of the amplitude time series for (**e**) EOF 1 and (**g**) EOF 2 are also shown. Amplitude time series indicate timing of particle release. Fraction of variance explained by EOFs 1 and 2 are shown in panels (**b**,**c**).

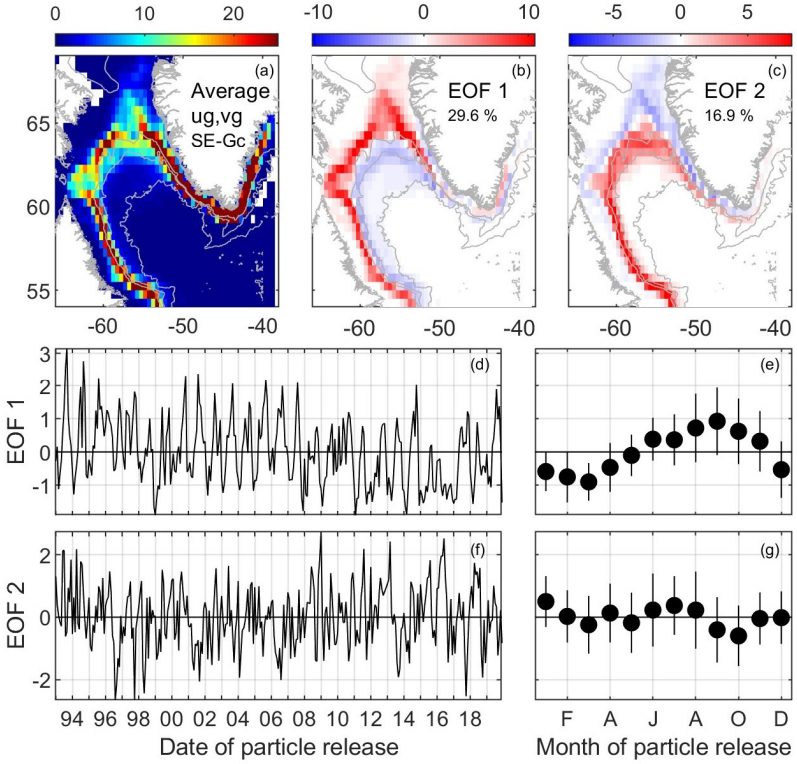

Figure 6. Heat maps showing distribution of particles released off southeast Greenland near the coast (SE−Gc) using only the geostrophic component of the velocity (ug, vg). (**a**) Average (%), (**b**) EOF 1 and (**c**) EOF 2, and amplitude time series for (**d**) EOF 1 and (**f**) EOF 2. Monthly averages of the amplitude time series for (**e**) EOF 1 and (**g**) EOF 2 are also shown. Amplitude time series indicate timing of particle release. Fraction of variance explained by EOFs 1 and 2 are shown in panels (**b**,**c**).

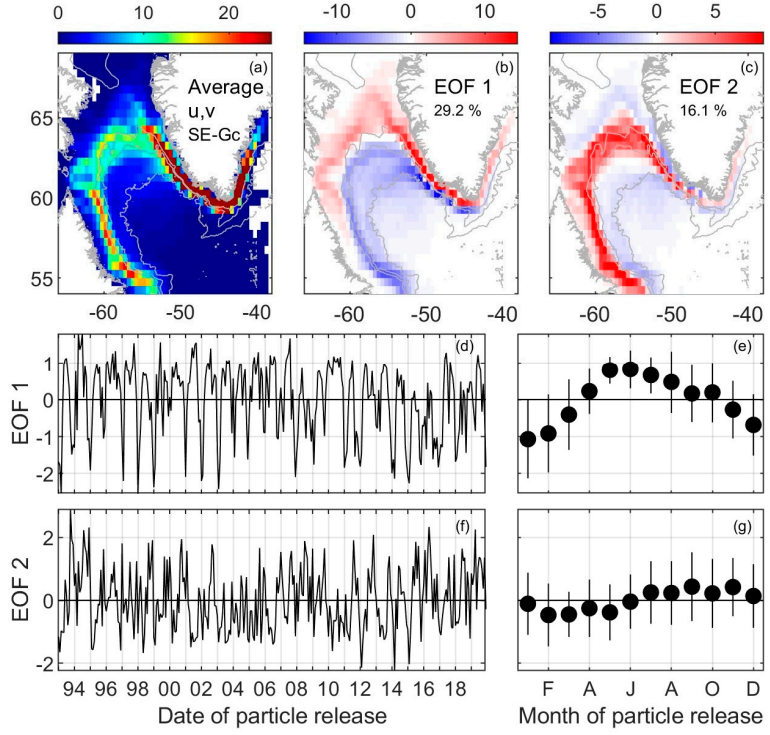

Figure 7. Heat maps showing distribution of particles released off southeast Greenland near the coast (SE−Gc) using total velocities including the wind effect (u, v). (**a**) Average (%), (**b**) EOF 1 and (**c**) EOF 2,

and amplitude time series for (**d**) EOF 1 and (**f**) EOF 2. Monthly averages of the amplitude time series for (**e**) EOF 1 and (**g**) EOF 2 are also shown. Amplitude time series indicate timing of particle release. Fraction of variance explained by EOFs 1 and 2 are shown in panels (**b**,**c**).

3.2. Westward Transport of Coastal Water in the Labrador Sea

The previous analysis revealed that transport pathways of coastal water in the Labrador Sea vary substantially, experiencing changes in the magnitude of the intensification as well as changes in their location and width. This indicates that the westward transport of water originating from coastal Greenland into the Labrador Sea will also vary. Histograms of the latitudes where particles move westward away from the southwest Greenland coast (i.e., the latitudes in which particles trajectories cross the magenta line shown in Figure 1b) are characterized by large seasonal variability (Figure 8). For particles released off southwest Greenland, westward transport occurs primarily to the north of 63°N (Figure 8a,b). Westward transport generally shifts a bit to the north for particles released in late summer and early fall, but the majority of the particles that move westward do so between 64 and 65°N (Figure 8a,b). A slight shift to the south is observed when total velocities are used in comparison to when only the geostrophic component is considered, especially for particles released in fall and winter (compare black and red lines in Figure 8c), when winds are predominantly upwelling-favorable on average (Figure 2).

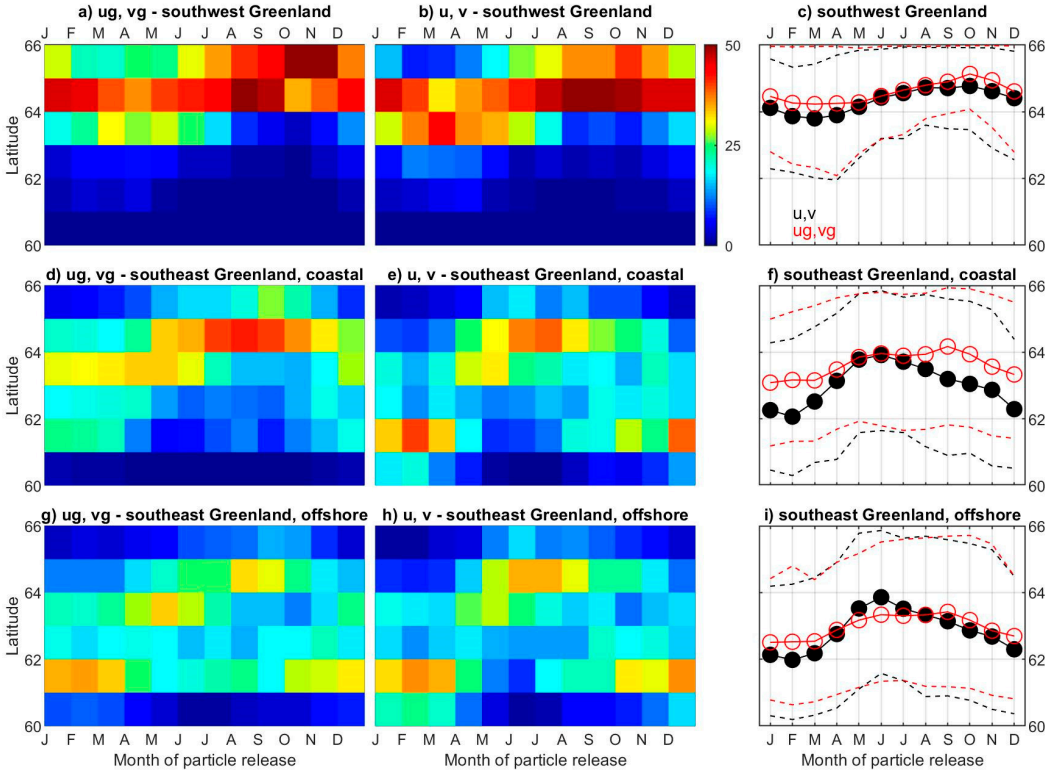

Figure 8. Histograms of latitude of westward displacement of particles across the magenta line shown in Figure 1b for particles released off (**a**,**b**) southwest Greenland, (**d**,**e**) coastal southeast Greenland, and (**g**,**h**) offshore southeast Greenland, using (**a**,**d**,**g**) only the geostrophic component of the flow or (**b**,**e**,**h**) total velocities including the wind-driven term. Only particles that move westward across the magenta line were considered, so that values in the various latitudinal bins for each month add to 100%. Time series of the weighted-averaged latitude of the westward movement for particles released in the three regions are shown in panels (**c**,**f**,**i**). Dashed lines show latitudinal band where 90% of the drifters moved westward across the magenta line (Figure 1b). In all cases, the *x*-axis indicates the timing of particle release.

For particles released off southeast Greenland, the seasonal shift in the latitude of crossing is more pronounced. For particles released near the coast, the offshore displacement for particles released in winter spans a large latitudinal band, from 61 to 65°N, peaking around 63–64°N when only geostrophic velocities are considered (Figure 8d). When total velocities are considered, transport around 61–62°N is intensified for particles released in winter (Figure 8e). In both cases, westward transport for particles released during summer occurs over a narrower latitudinal band, around 64–65°N, when only the geostrophic component is considered, and around 63–65°N when total velocities are considered. Except for particles released from May to July, including the wind effect results in particles moving westward into the basin farther to the south compared to when only the geostrophic component is considered (Figure 8f). Lastly, for particles released farther offshore from the southeast Greenland coast, a similar seasonal cycle (compared to those released near the coast) is observed, although westward transport occurs over a broad latitudinal band throughout the year (Figure 8g–i).

3.3. Spatial and Temporal Variability in Source Water in Different Regions of the Labrador Sea

Different regions in the Labrador Sea may be impacted differently by water from coastal regions off Greenland, depending on the time of year. Here, we look at how the source water for five different regions (shown in Figure 1b) varies seasonally (Figure 9), as well as how it varies between the years for water introduced near the coast during the melting season (Figures 10–12). On average, the majority of particles released off southwest Greenland are either transported toward Baffin Bay or they become grounded along the southwest Greenland coast soon after release as they are transported northward. That pattern is observed year round when only geostrophic velocities are considered (Figure 9a, dashed blue). When total velocities including the wind component are considered, this pattern is observed primarily for particles released from May to August, which includes the peak melting season (Figure 9a, solid blue). For particles released in fall and winter, when coastal winds off southwest Greenland are generally southward (Figure 2), there is a substantial decrease in the fraction of particles released off southwest Greenland that are transported to Baffin Bay or that become grounded. A somewhat similar pattern is observed for particles released off southeastern Greenland (Figure 9a, red and green lines), although the fraction of particles moving into Baffin Bay or becoming grounded off southwest Greenland is smaller, especially for particles released farther from the coast. Wind forcing tends to increase northward transport and/or grounding for particles released from April to June and to decrease it during the rest of the year. The increase in northward transport for particles released from April to June occurs approximately 2 months earlier than the increase observed for particles released off southwest Greenland, agreeing with Luo et al. [29], which showed that it takes, on average, about 2 months for water from southeast Greenland to be transported toward southwest Greenland. Farther south, in the central Labrador Sea and in the convection region (see Figure 1b for locations), very few particles released off southwest Greenland are observed (Figure 9d,e). In contrast, water from near the coast off southeast Greenland is more likely to be transported toward those regions (see Figure 3 for an example). That is especially true for particles released in late fall and winter when total velocities are considered. The seasonality is reduced when wind forcing is not considered (compare solid and dashed red lines in Figure 9d,e). A similar pattern is observed for particles released farther offshore off southeast Greenland, with the percentage of particles moving into the interior of the Labrador Sea being slightly larger than for particles released near the coast (compare red and green lines in Figure 9d,e).

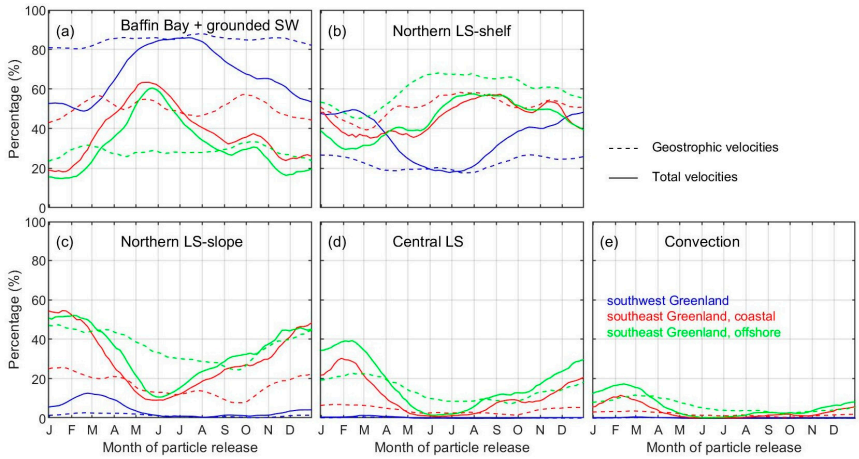

Figure 9. Time series of monthly averages of the percentage of particles released off southwest Greenland (blue) or southeast Greenland (near the coast in red, offshore in green) that reached each of the 5 regions shown in Figure 1b ((**a**)—Baffin Bay + grounded SW; (**b**)—northern Labrador Sea shelf; (**c**)—northern Labrador Sea slope; (**d**)—central Labrador Sea; (**e**)—convection region.). Percentages using total velocities are shown by solid lines, while dashed lines were computed when only the geostrophic component of the flow was used. In all cases, the *x*-axis indicates the timing of particle release.

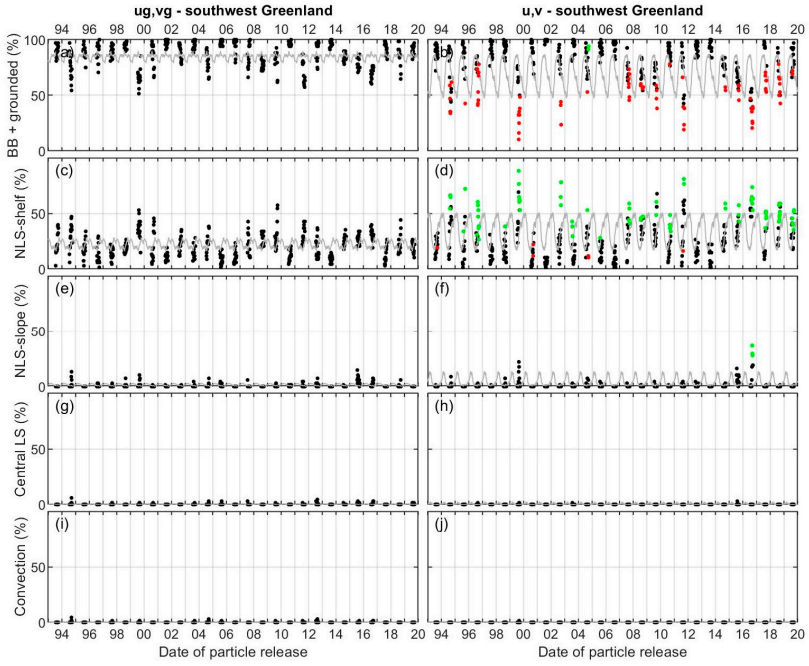

Figure 10. Time series of the percentage of particles released during the melting season off southwest Greenland that were transported into the 5 regions identified in Figure 1b ((**a**,**b**)—Baffin Bay + grounded SW; (**c**,**d**)—northern Labrador Sea shelf; (**e**,**f**)—northern Labrador Sea slope; (**g**,**h**)—central Labrador Sea; (**i**,**j**)—convection region) using (left) only the geostrophic component of the flow or (right) total velocities including the wind component. When only geostrophic velocities were used (i.e., left panels), the percentages for each year are shown by the small black dots. When total velocities were used (i.e., right panels), percentages are also shown by small black dots, except when the percentages are at least 20 percentage points smaller (red) or larger (green) than the percentage computed using only the geostrophic flow. Monthly averages over the entire year (from Figure 9) are shown in gray. In all cases, the *x*-axis indicates the timing of particle release.

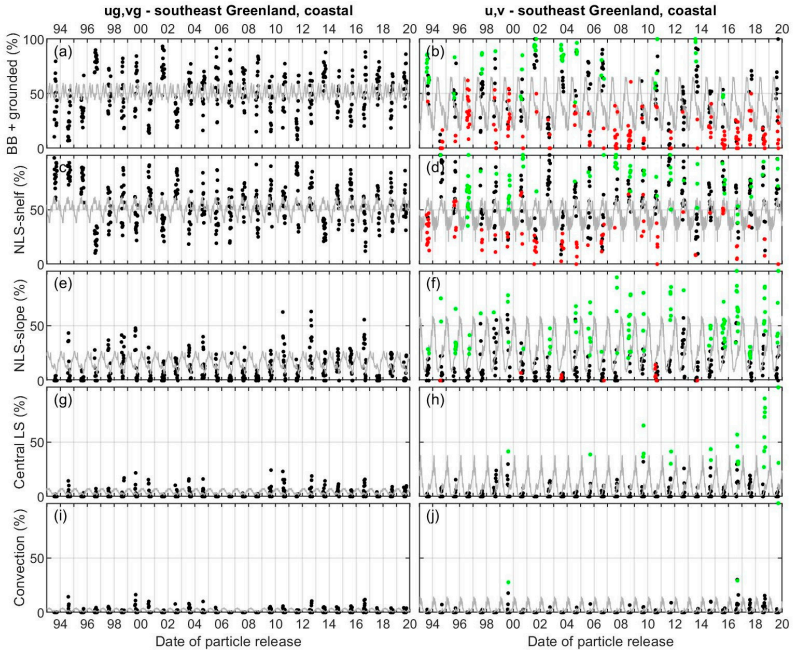

Figure 11. Same as Figure 10, but for particles released during the melting season near the coast off southeast Greenland.

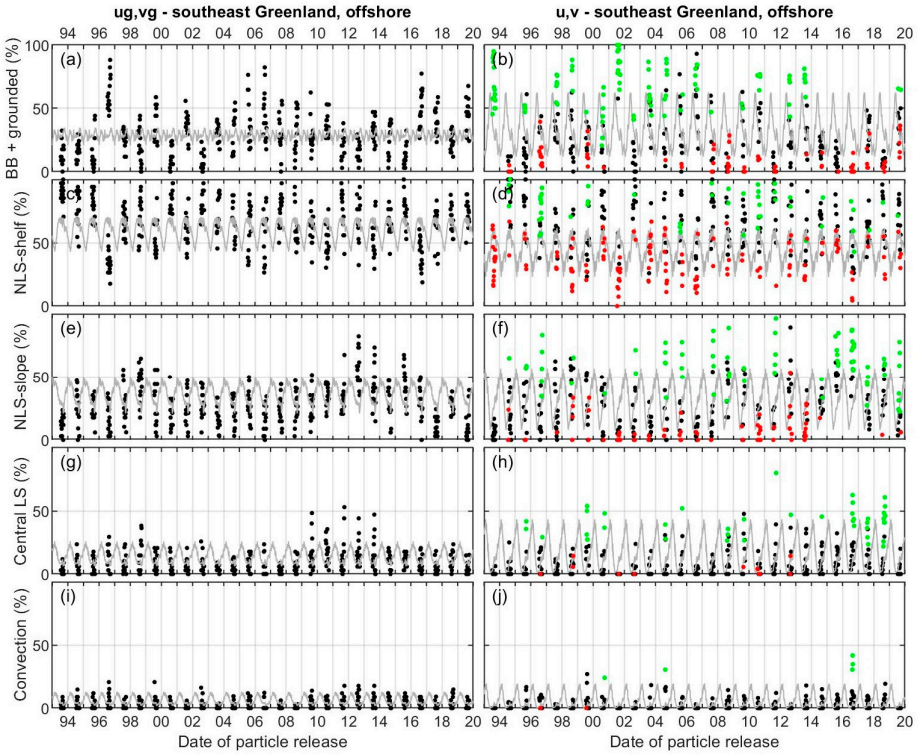

Figure 12. Same as Figure 10, but for particles released during the melting season offshore off southeast Greenland.

We split the area to the north of the 3000 m isobath and to the south of Baffin Bay into two regions (Figure 1b). We used the 2000 m isobath as the divide, given that the average distribution of particles is generally enhanced to the north of that isobath (see panel a in Figures 4–7). The behavior of particles released off southeast Greenland is generally out of phase in those two regions (Figure 9b,c). Particles released in late fall and winter are more

frequently observed in the northern LS slope, while particles released during summer are more frequently observed farther north in the northern LS shelf. This is consistent with the histograms of the latitude of westward displacements of particles in the Labrador Sea that were released off southeast Greenland, which were characterized by a northward shift during summer and a southward shift during winter (Figure 8d–i). Including the wind effect generally results in a reduction in the number of particles from southeast Greenland that are transported into the northern LS shelf (Figure 9b). For the northern LS slope, the opposite is observed for particles released off coastal southeast Greenland, whose transport is increased in fall and winter when total velocities are considered (compare solid and dashed red lines in Figure 9c).

Given our interest in the potential effects of meltwater from the Greenland ice sheet in the Labrador Sea, we also plot time series of the fraction of particles released during the melting season (mid-July to September) that reach each of the five regions described above during the 27 years analyzed here (Figures 10–12). For particles released off southwest Greenland during the melting season, most are either transported to Baffin Bay (or become grounded) or to the northern LS shelf depending on the year (Figure 10). Substantial interannual variability is observed, even when only geostrophic velocities are considered (Figure 10a,c). Adding the wind effect generally results in fewer particles being transported toward Baffin Bay or becoming grounded and more being transported to the northern LS shelf in several of the years considered here (Figure 10b,d). Very few particles released during the melting season are transported to the northern LS slope, and virtually none are transported into the central Labrador Sea and the convection region (Figure 10e–j). In the northern LS shelf, a linear fit (significant at the 95% confidence level) reveals an increase in the transport of particles released during the melting season of 4.9% per decade when total velocities are considered (Table 1).

Table 1. Temporal trends (i.e., slope coefficient of the regression, $y = at + b$, where t is time; in % per decade) for the fraction of particles released during the melting season off southwest Greenland, coastal and offshore southeast Greenland that reached each of the 5 regions shown in Figure 1b when total velocities including the wind-driven term are considered.

Total Velocities (u, v)	Southwest Greenland	Southeast Greenland, Coastal	Southeast Greenland, Offshore
Baffin Bay + grounded SW	−4.0 *	−7.9 *	−8.1 *
Northern LS—shelf	4.9 *	1.6	0.6
Northern LS—slope	0.6 *	8.5 *	9.1 *
Central LS	0.0	4.9 *	5.1 *
Convection region	0.0	1.4 *	1.1 *

* value is significant at the 95% confidence level.

Our previous analysis revealed that particles released off southeast Greenland are transported westward into the Labrador Sea over a broad latitudinal range (Figure 8d–i). Most of the particles released near the coast during the melting season are transported toward Baffin Bay and the northern Labrador Sea shelf and slope (Figure 11a–f). Once again, using total velocities including the wind-driven term generally results in particles being transported westward farther to the south in several years, so that, in general, fewer particles reach Baffin Bay or become grounded off southwest Greenland, and more are transported into the northern LS slope (Figure 11b,f) compared to when only geostrophic velocities are considered. Interannual variability is quite large, with an anomalously large fraction of particles being transported into the northern LS slope in 2007–2009, 2011, 2016, and 2018. While the frequency of particles transported into the northern LS slope seems to be increasing (8.5%/decade; Table 1), the frequency of those transported to Baffin Bay or that become grounded seems to be decreasing (−7.9%/decade; Table 1). Although very

few particles released off coastal southeast Greenland during the melting season reach the central Labrador Sea on average (Figure 9d), effective transport does occur in some years, such as in 2009, 2016, and 2018 (Figure 11h; linear trend of 4.9%/decade; Table 1). Slightly increased transport toward the convection region was observed in 2016–2018 (Figure 11j).

Lastly, for particles released farther offshore off southeast Greenland during the melting season (Figure 12), a similar pattern is observed, except that the westward transport off southwest Greenland generally occurs slightly to the south (Figure 8). As a result, more particles are transported toward the central Labrador Sea and the convection region (Figure 12g–j). The net effect of winds along the entire trajectories can be to either increase or decrease the fraction of the particles that reach Baffin Bay or become grounded compared to when only geostrophy is considered, depending on the year (Figure 12b), and to increase the fraction of those that reach the northern LS slope in most years (Figure 12f). Linear trends when total velocities are considered reveal a temporal decrease in the number of particles reaching Baffin Bay or becoming grounded (−8.1%/decade) and an increase in the percentage reaching the northern LS slope, the central Labrador Sea, and the convection region (9.1, 5.1 and 1.1% per decade, respectively; Table 1).

4. Discussion and Conclusions

Transport processes in the Labrador Sea have been the focus of many studies over the last few decades. More recently, particular attention has been given to the fate of meltwater from the Greenland ice sheet. The majority of these previous studies relied on model simulations. Here, we expand on those studies by using 27 years of satellite altimetry observations modified to include wind effects via Ekman dynamics [32] to investigate spatial and temporal variability in the transport of coastal water from southwest and southeast Greenland in the Labrador Sea. Altimetry observations have been shown to accurately represent the nature of the flow over the shelf off south Greenland, allowing for long-term studies of circulation in the region based on satellite data [37]. Our results revealed that most particles released off Greenland are transported around the Labrador Sea approximately following isobaths, or to the north toward Baffin Bay, consistent with previous investigations [13,26,29]. Our results are also consistent with previous studies that have shown that the fate of coastal water off Greenland in the Labrador Sea is strongly influenced by wind effects [27,29,31]. However, the virtual drifter trajectories also showed that clear seasonality in transport pathways is observed, even when only geostrophic velocities from altimetry are considered. In particular, trajectories of drifters moving westward into the Labrador Sea are generally displaced to the south during winter and to the north during summer, even in the absence of wind effects. That pattern is generally reinforced when wind forcing is considered, although winds can also modify the timing of peak transport along a pathway.

In addition to investigating seasonality, the use of a long time series spanning 27 years allowed us to investigate interannual variability in the fate of the coastal water that is found off south Greenland during summer and is, thus, influenced by melting of the Greenland ice sheet. Although coastal water found off southwest Greenland during summer is mostly transported toward Baffin Bay or remains very near the southwest Greenland coast (which is consistent with Luo et al. [29]), increased westward transport in the region, referred to here as the northern Labrador Sea shelf, is observed in several years, associated with anomalously upwelling-favorable winds during summer. A progressive decrease in the fraction of the meltwater-influenced coastal water from southwest Greenland that is transported toward Baffin Bay and a progressive increase in the fraction that is transported westward were observed when wind effects were included (Table 1; trends were not significant when only geostrophic velocities were used), which may have important biogeochemical implications. Meltwater input can influence nutrient distribution, either by supplying some nutrients [16,17,42] or by diluting ocean nutrient levels in the case of nutrient-poor meltwater [43–45], also contributing to phytoplankton growth by changing local stratification and pycnocline depth during fall [20]. This suggests that progressive

changes in the fate of the meltwater from southwest Greenland could have implications for the spatial distribution of phytoplankton abundance off west Greenland. Even though westward transport of coastal water off southwest Greenland influenced by meltwater may be slowly increasing, essentially no particles were transported to the convection region in any of the 27 years considered here, supporting earlier modeling studies [31] and suggesting little implication for winter convection.

Water from southeast Greenland is known to be more efficiently transported westward away from the coast into the Labrador Sea [29–31]. Indeed, up to 20–40% of the drifters released off southeast Greenland in fall and winter (when winds off southwest Greenland are predominantly upwelling favorable) and that moved westward beyond the southern tip of Greenland can be transported into the central Labrador Sea. Many fewer of those drifters reach the central Labrador Sea when wind effects are not considered, indicating the critical role played by winds in the process, which is consistent with [27]. Most of the particles transported toward the convection region are released in winter, when the impact of meltwater input from the Greenland ice sheet in the coastal ocean is small. Freshwater transport off east Greenland associated with water from the Arctic peaks in December–March [7], however, suggesting that some of that Arctic freshwater may be transported toward the interior of the basin. Even though water found near the southeast coast during summer, when meltwater input from the Greenland ice sheet is largest, is generally not transported toward the central Labrador Sea (Figure 9d,e; see also Figure 6a in [27]), our results show that it can be transported to the interior of the basin in some years, especially when the wind forcing is considered, sometimes even reaching the convection region (Figure 11j). Furthermore, linear trends are positive and significant, suggesting a potential increase in the transport of coastal water found off southeast Greenland during summer toward the central Labrador Sea and the convection region during the 27 years studied here. More meltwater transport toward the interior of the basin could, thus, affect local water stability in the convection region. However, the increase in the transport toward the convection region is only significant when total velocities including the wind effect are considered. This is important because most of the freshwater from Greenland ice sheet melting off southeast Greenland is actually introduced into fjords at the subsurface at marine-terminating glaciers [46]. The buoyant upwelled meltwater generally becomes neutrally buoyant at the subsurface and travels toward the mouth of the fjord at the depth of neutral buoyancy [47]. Although these processes are influenced by a variety of factors, including the fjord geometry [48,49], the export of the meltwater from the fjords into the coastal ocean generally occurs at the subsurface [50], where it will be sheltered from direct wind effects. If the meltwater remains at the subsurface as it is transported in the East Greenland Current around the southern tip of Greenland into the Labrador Sea, then our estimates of transport toward the central Labrador Sea and the convection region considering the wind effect (Figure 11h,j) would be less relevant. In that case, estimates using geostrophic velocities (Figure 11g,i) could be more appropriate, in which case, even though some of the coastal water reaches the convection region, no significant temporal trend was observed. Better constraining the role played by winds on the fate of meltwater plumes from southeast Greenland in the Labrador Sea is also important for biological processes, since those plumes are likely to be enriched in nutrients due to buoyancy-driven upwelling inside fjords [19,50], possibly playing a key role in the development of phytoplankton summer blooms off west Greenland [5].

Offshore water off southeast Greenland during summer is more efficiently transported toward the central Labrador Sea [27] and even toward the convection region. In situ and satellite observations [39] and model results [27] indicate that the offshore water is generally substantially saltier than water found near the coast during summer, however, so its potential for increasing stratification in the convection regions is comparatively smaller.

A limitation of the present study is that some of the particles released in the coastal ocean were transported toward the shore, becoming grounded. Particles that move onshore off southwest Greenland are generally associated with downwelling-favorable winds and,

thus, with northward transport toward Baffin Bay [29,31]. Because of that, particles that became grounded off southwest Greenland and those that reached Baffin Bay were grouped together in Figures 9a, 10, 11 and 12a,b, capturing particles that did not move westward away from the coast to the south of 66°N. Even though grounding is not a realistic behavior for a meltwater plume or a water parcel [51], the approach described above produced results consistent with those described in Luo et al. [29], using a passive tracer, and allowed for interannual variability in transport to be assessed. Another limitation is the use of low-resolution altimetry observations [52] to compute the geostrophic component of the flow, which do not allow for capturing the small-scale variability that is known to play a key role in the transport of materials in the ocean [53]. The transport of low-salinity waters from the West Greenland Current into the interior of the Labrador Sea is thought to be influenced by small mesoscale eddies associated with instabilities in the West Greenland Current [23,54]. Resolving small-scale processes is especially important in high-latitude regions such as the Labrador Sea, where the spatial scales of variability are reduced, and submesoscale vortices have been shown to contribute significantly to cross-isobath transport [28]. Given the relatively low resolution of altimetry data, these processes are not properly represented in the analyses presented here. Satellite observations that are now being obtained in higher resolution as part of NASA's Surface Water and Ocean Topography mission (SWOT; [55,56]) have the potential to be used to quantify the role of submesoscale processes on transport pathways in the Labrador Sea. Lastly, recent studies have indicated that considering the impact of wave-induced Stokes drift on ocean surface currents can result in improved representation of in situ Lagrangian drifter currents [57] and in modified transport pathways [58–60]. These point out the importance of quantifying if and how Stokes drift may impact the coastal transport pathways identified here.

Author Contributions: Conceptualization, R.M.C., H.O. and P.M.M.; methodology, R.M.C., H.O. and P.M.M.; formal analysis, R.M.C.; investigation, R.M.C.; writing—original draft preparation, R.M.C.; writing—review and editing, R.M.C., H.O. and P.M.M.; funding acquisition, R.M.C., H.O. and P.M.M. All authors have read and agreed to the published version of the manuscript.

Funding: This research was funded by NSF (OCE-2219874; OCE-2212654) and NASA Physical Oceanography Program.

Data Availability Statement: Publicly available datasets were analyzed in this study. OSCAR is generated by Earth & Space Research (ESR; https://www.esr.org/research/oscar), and it can be downloaded at PO.DAAC (https://doi.org/10.5067/OSCAR-25F20, accessed on 20 November 2022). CCMP Version-3.0 vector wind analyses are produced by Remote Sensing Systems. Data are available at www.remss.com (accessed on 17 August 2023). Parcels is available at https://oceanparcels.org (accessed on 20 November 2022).

Acknowledgments: The authors thank the anonymous reviewers for their comments and suggestions, which resulted in an improved manuscript.

Conflicts of Interest: The authors declare no conflict of interest. The funders had no role in the design of the study; in the collection, analyses, or interpretation of data; in the writing of the manuscript; or in the decision to publish the results.

References

1. Nielsen, J. *The Waters around Greenland. Greenland: The Discovery of Greenland, Exploration, and the Nature of the Country*; Vahl, M., Rietzel, C.A., Eds.; Oxford University Press Publisher: Oxford, UK, 1928; Volume I, pp. 185–230.
2. Smith, E.H.; Soule, F.M.; Mosby, O. The Marion and General Greene expeditions to Davis Strait and Labrador Sea. Scientific Results, Part 2, Physical Oceanography. *Bull. U.S. Coast Guard* **1937**, *19*, 1–259.
3. Lazier, J.R.N. The renewal of Labrador Sea water. *Deep. Sea Res. Oceanogr. Abstr.* **1973**, *20*, 341–353. [CrossRef]
4. Wu, Y.; Platt, T.; Tang, C.C.; Sathyendranath, S. Regional differences in the timing of the spring bloom in the Labrador Sea. *Mar. Ecol. Prog. Ser.* **2008**, *355*, 9–20. [CrossRef]
5. Arrigo, K.R.; van Dijken, G.L.; Castelao, R.M.; Luo, H.; Rennermalm, Å.K.; Tedesco, M.; Mote, T.L.; Oliver, H.; Yager, P.L. Melting glaciers stimulate large summer phytoplankton blooms in southwest Greenland waters. *Geophys. Res. Lett.* **2017**, *44*, 6278–6285. [CrossRef]

6. Foukal, N.P.; Gelderloos, R.; Pickart, R.S. A continuous pathway for fresh water along the East Greenland shelf. *Sci. Adv.* **2020**, *6*, eabc4254. [CrossRef] [PubMed]
7. Le Bras, I.A.-A.; Straneo, F.; Holte, J.; Holliday, N.P. Seasonality of freshwater in the East Greenland Current system from 2014 to 2016. *J. Geophys. Res. Ocean.* **2018**, *123*, 8828–8848. [CrossRef]
8. Rignot, E.; Box, J.E.; Burgess, E.; Hanna, E. Mass balance of the Greenland ice sheet from 1958 to 2007. *Geophys. Res. Lett.* **2008**, *35*, L20502. [CrossRef]
9. Shepherd, A.; Ivins, E.R.; Barletta, V.R.; Bentley, M.J.; Bettadpur, S.; Briggs, K.H.; Bromwich, D.H.; Forsberg, R.; Galin, N.; Horwath, M.; et al. A reconciled estimate of ice-sheet mass balance. *Science* **2012**, *338*, 1183–1189. [CrossRef]
10. Bamber, J.; van den Broeke, M.; Ettema, J.; Lenaerts, J.; Rignot, E. Recent large increases in freshwater fluxes from Greenland into the North Atlantic. *Geophys. Res. Lett.* **2012**, *39*, L19501. [CrossRef]
11. Bamber, J.L.; Tedstone, A.J.; King, M.D.; Howat, I.M.; Enderlin, E.M.; van den Broeke, M.R.; Noel, B. Land ice freshwater budget of the Arctic and North Atlantic Oceans: 1. Data, methods, and results. *J. Geophys. Res. Ocean.* **2018**, *123*, 1827–1837. [CrossRef]
12. The IMBIE Team. Mass balance of the Greenland Ice Sheet from 1992 to 2018. *Nature* **2020**, *579*, 233–239.
13. Böning, C.; Behrens, E.; Biastoch, A.; Getzlaff, K.; Bamber, J. Emerging impact of Greenland meltwater on deepwater formation in the North Atlantic Ocean. *Nat. Geosci.* **2016**, *9*, 523–528. [CrossRef]
14. Rahmstorf, S.; Box, J.; Feulner, G.; Mann, M.; Robinson, A.; Rutherford, S.; Schaffernicht, E. Exceptional twentieth-century slowdown in Atlantic Ocean overturning circulation. *Nat. Clim. Change* **2015**, *5*, 475–480. [CrossRef]
15. Caesar, L.; Rahmstorf, S.; Robinson, A.; Feulner, G.; Saba, V. Observed fingerprint of a weakening Atlantic Ocean overturning circulation. *Nature* **2018**, *556*, 191–196. [CrossRef] [PubMed]
16. Bhatia, M.P.; Kujawinski, E.B.; Das, S.B.; Breier, C.F.; Henderson, P.B.; Charette, M.A. Greenland meltwater as a significant and potentially bioavailable source of iron to the ocean. *Nat. Geosci.* **2013**, *6*, 274–278. [CrossRef]
17. Hawkings, J.R.; Wadham, J.L.; Tranter, M.; Raiswell, R.; Benning, L.G.; Statham, P.J.; Tedstone, A.; Nienow, P.; Lee, K.; Telling, J. Ice sheets as a significant source of highly reactive nanoparticulate iron to the oceans. *Nat. Commun.* **2014**, *5*, 3929. [CrossRef] [PubMed]
18. Hawkings, J.R.; Wadham, J.L.; Tranter, M.; Lawson, E.; Sole, A.; Cowton, T.; Tedstone, A.J.; Bartholomew, I.; Niewnow, P.; Chandler, D.; et al. The effect of warming climate on nutrient and solute export from the Greenland Ice Sheet. *Geochem. Perspect. Lett.* **2015**, *1*, 94–104. [CrossRef]
19. Hopwood, M.J.; Carroll, D.; Browning, T.J.; Meire, L.; Mortensen, J.; Krisch, S.; Achterberg, E.P. Non-linear response of summertime marine productivity to increased meltwater discharge around Greenland. *Nat. Commun.* **2018**, *9*, 3256. [CrossRef]
20. Oliver, H.; Luo, H.; Castelao, R.M.; van Dijken, G.L.; Mattingly, K.S.; Rosen, J.J.; Mote, T.L.; Arrigo, K.R.; Rennermalm, Å.K.; Tedesco, M.; et al. Exploring the potential impact of Greenland meltwater on stratification, photosynthetically active radiation, and primary production in the Labrador Sea. *J. Geophys. Res. Ocean.* **2018**, *123*, 2570–2591. [CrossRef]
21. Pickart, R.S.; Torres, D.J.; Clarke, R.A. Hydrography of the Labrador Sea during active convection. *J. Phys. Oceanogr.* **2002**, *32*, 428–457. [CrossRef]
22. Cuny, J.; Rhines, P.B.; Niiler, P.P.; Bacon, S. Labrador Sea boundary currents and the fate of the Irminger Sea Water. *J. Phys. Oceanogr.* **2002**, *32*, 627–647. [CrossRef]
23. Prater, M.D. Eddies in the Labrador Sea as observed by profiling RAFOS floats and remote sensing. *J. Phys. Oceanogr.* **2002**, *32*, 411–427. [CrossRef]
24. Straneo, F. Heat and freshwater Transport through the central Labrador Sea. *J. Phys. Oceanogr.* **2006**, *36*, 606–628. [CrossRef]
25. Swingedouw, D.; Rodehacke, C.B.; Behrens, E.; Menary, M.; Olsen, S.M.; Gao, Y.; Mikolajewicz, U.; Mignot, J.; Biastoch, A. Decadal fingerprints of freshwater discharge around Greenland in a multi-model ensemble. *Clim. Dyn.* **2013**, *41*, 695–720. [CrossRef]
26. Dukhovskoy, D.S.; Myers, P.G.; Platov, G.; Timmermans, M.; Curry, B.; Proshutinsky, A.; Bamber, J.L.; Chassignet, E.; Hu, X.; Lee, C.M.; et al. Greenland freshwater pathways in the sub-Arctic seas from model experiments with passive tracers. *J. Geophys. Res. Oceans* **2016**, *121*, 877–907. [CrossRef]
27. Chretien, L.M.S.; Frajka-Williams, E. Wind-driven transport of fresh shelf water into the upper 30 m of the Labrador Sea. *Ocean Sci.* **2018**, *14*, 1247–1264. [CrossRef]
28. Tagklis, F.; Bracco, A.; Ito, T.; Castelao, R.M. Submesoscale modulation of deep water formation in the Labrador Sea. *Sci. Rep.* **2020**, *10*, 1–13. [CrossRef]
29. Luo, H.; Castelao, R.M.; Rennermalm, A.K.; Tedesco, M.; Bracco, A.; Yager, P.L.; Mote, T.L. Oceanic transport of surface meltwater from the southern Greenland ice sheet. *Nat. Geosci.* **2016**, *9*, 528–532. [CrossRef]
30. Gillard, L.C.; Hu, X.; Myers, P.G.; Bamber, J.L. Meltwater pathways from marine terminating glaciers of the Greenland ice sheet. *Geophys. Res. Lett.* **2016**, *43*, 10873–10882. [CrossRef]
31. Castelao, R.M.; Luo, H.; Oliver, H.; Rennermalm, A.K.; Tedesco, M.; Bracco, A.; Yager, P.L.; Mote, T.L.; Medeiros, P.M. Controls on the transport of meltwater from the southern Greenland ice sheet in the Labrador Sea. *J. Geophys. Res. Oceans* **2019**, *124*, 3551–3560. [CrossRef]
32. Bonjean, F.; Lagerloef, G.S.E. Diagnostic model and analysis of the surface currents in the tropical Pacific Ocean. *J. Phys. Oceanogr.* **2020**, *32*, 2938–2954. [CrossRef]
33. Delandmeter, P.; van Sebille, E. The Parcels v2.0 Lagrangian framework: New field interpolation schemes. *Geosci. Model Dev.* **2019**, *12*, 3571–3584. [CrossRef]

34. Castelao, R.M.; Medeiros, P.M. Coastal Summer Freshening and Meltwater Input off West Greenland from Satellite Observations. *Remote Sens.* **2022**, *14*, 6069. [CrossRef]
35. Hersbach, H.; Bell, B.; Berrisford, P.; Biavati, G.; Horányi, A.; Muñoz Sabater, J.; Nicolas, J.; Peubey, C.; Radu, R.; Rozum, I.; et al. *ERA5 Hourly Data on Single Levels from 1979 to Present*; Copernicus Climate Change Service (C3S); Climate Data Store (CDS); European Commission: Brussels, Belgium, 2018. [CrossRef]
36. Van Sebille, E.; Griffies, S.M.; Abernathey, R.; Adams, T.P.; Berloff, P.; Biastoch, A.; Blanke, B.; Chassignet, E.P.; Cheng, Y.; Cotter, C.J.; et al. Lagrangian ocean analysis: Fundamentals and practices. *Ocean Model.* **2018**, *121*, 49–75. [CrossRef]
37. Coquereau, A.; Foukal, N.P. Evaluating altimetry-derived surface currents on the south Greenland shelf with surface drifters. *Ocean Sci.* **2023**, *19*, 1393–1411. [CrossRef]
38. Myers, P.G.; Donnelly, C.; Ribergaard, M.H. Structure and variability of the West Greenland Current in summer derived from 6 repeat standard sections. *Prog. Oceanogr.* **2009**, *80*, 93–112. [CrossRef]
39. Majumder, S.; Castelao, R.M.; Amos, C.M. Freshwater variability and transport in the Labrador Sea from in situ and satellite observations. *J. Geophys. Res. Oceans* **2021**, *126*, e2020JC016751. [CrossRef]
40. Mears, C.; Lee, T.; Ricciardulli, L.; Wang, X.; Wentz, F. *RSS Cross-Calibrated Multi-Platform (CCMP) 6-Hourly Ocean Vector Wind Analysis on 0.25 Deg Grid, Version 3.0*; Remote Sensing Systems: Santa Rosa, CA, USA, 2022. [CrossRef]
41. Barth, J.A.; Menge, B.A.; Lubchenco, J.; Chan, F.; Bane, J.M.; Kirincich, A.R.; McManus, M.A.; Nielsen, K.J.; Pierce, S.D.; Washburn, L. Delayed upwelling alters nearshore coastal ocean ecosystems in the northern California current. *Proc. Natl. Acad. Sci. USA* **2007**, *104*, 3719–3724. [CrossRef]
42. Wadham, J.L.; Hawkings, J.; Telling, J.; Chandler, D.; Alcock, J.; O'Donnell, E.; Kaur, P.; Bagshaw, E.; Tranter, M.; Tedstone, A.; et al. Sources, cycling and export of nitrogen on the Greenland Ice Sheet. *Biogeosciences* **2016**, *13*, 6339–6352. [CrossRef]
43. Hopwood, M.J.; Bacon, S.; Arendt, K.; Connelly, D.P.; Statham, P.J. Glacial meltwater from Greenland is not likely to be an important source of Fe to the North Atlantic. *Biogeochemistry* **2015**, *124*, 1–11. [CrossRef]
44. Hopwood, M.J.; Connelly, D.P.; Arendt, K.E.; Juul-Pedersen, T.; Stinchcombe, M.C.; Meire, L.; Esposito, M.; Krishna, R. Seasonal changes in Fe along a glaciated Greenlandic Fjord. *Front. Earth Sci.* **2016**, *4*, 15. [CrossRef]
45. Meire, L.; Mortensen, J.; Meire, P.; Juul-Pedersen, T.; Sejr, M.K.; Rysgaard, S.; Nygaard, R.; Huybrechts, P.; Meysman, F.J.R. Marine-terminating glaciers sustain high productivity in Greenland fjords. *Glob. Change Biol.* **2017**, *23*, 5344–5357. [CrossRef] [PubMed]
46. Slater, D.A.; Straneo, F.; Felikson, D.; Little, C.M.; Goelzer, H.; Fettweis, X.; Holte, J. Estimating Greenland tidewater glacier retreat driven by submarine melting. *Cryosphere* **2019**, *13*, 2489–2509. [CrossRef]
47. Straneo, F.; Cenedese, C. The dynamics of Greenland's glacial fjords and their role in climate. *Annu. Rev. Mar. Sci.* **2015**, *7*, 89–112. [CrossRef] [PubMed]
48. Carroll, D.; Sutherland, D.A.; Hudson, B.; Moon, T.; Catania, G.A.; Shroyer, E.L.; Nash, J.D.; Bartholomaus, T.C.; Felikson, D.; Stearns, L.A.; et al. The impact of glacier geometry on meltwater plume structure and submarine melt in Greenland fjords. *Geophys. Res. Lett.* **2016**, *43*, 9739–9748. [CrossRef]
49. Carroll, D.; Sutherland, D.A.; Shroyer, E.L.; Nash, J.D.; Catania, G.A.; Stearns, L.A. Subglacial discharge-driven renewal of tidewater glacier fjords. *J. Geophys. Res. Oceans* **2017**, *122*, 6611–6629. [CrossRef]
50. Oliver, H.; Castelao, R.M.; Wang, C.; Yager, P.L. Meltwater-enhanced nutrient export from Greenland's glacial fjords: A sensitivity analysis. *J. Geophys. Res. Oceans* **2020**, *125*, e2020JC01618. [CrossRef]
51. Pawlowicz, R.; Hannah, C.; Rosenberger, A. Lagrangian observations of estuarine residence times, dispersion, and trapping in the Salish Sea. *Estuar. Coast. Shelf Sci.* **2019**, *225*, 106246. [CrossRef]
52. Chelton, D.B.; Schlax, M.G.; Samelson, R.M. Global observations of nonlinear mesoscale eddies. *Prog. Oceanogr.* **2011**, *91*, 167–216. [CrossRef]
53. McWilliams, J.C. Submesoscale currents in the ocean. *Proc. R. Soc. A Math. Phys. Eng. Sci.* **2016**, *472*, 20160117. [CrossRef]
54. Lilly, J.M.; Rhines, P.B.; Schott, F.; Lavender, K.; Lazier, J.; Send, U.; D'asaro, E. Observations of the Labrador Sea eddy field. *Prog. Oceanogr.* **2003**, *59*, 75–176. [CrossRef]
55. Fu, L.-L.; Alsdorf, D.; Morrow, R.; Rodriguez, E.; Mognard, N. SWOT: The Surface Water and Ocean Topography Mission—Wideswath Altimetric Measurement of Water Elevation on Earth. NASA. 2012. Available online: https://trs.jpl.nasa.gov/handle/2014/41996 (accessed on 20 November 2022).
56. Morrow, R.; Fu, L.-L.; Ardhuin, F.; Benkiran, M.; Chapron, B.; Cosme, E.; D'ovidio, F.; Farrar, J.T.; Gille, S.T.; Lapeyre, G.; et al. Global Observations of Fine-Scale Ocean Surface Topography with the Surface Water and Ocean Topography (SWOT) Mission. *Front. Mar. Sci.* **2019**, *6*, 232. [CrossRef]
57. Hui, Z.; Xu, Y. The impact of wave-induced Coriolis-Stokes forcing on satellite-derived ocean surface currents. *J. Geophys. Res. Oceans* **2016**, *121*, 410–426. [CrossRef]
58. Ardhuin, F.; Marié, L.; Rascle, N.; Forget, P.; Roland, A. Observation and estimation of Lagrangian, Stokes and Eulerian currents induced by wind and waves at the sea surface. *J. Phys. Oceanogr.* **2019**, *39*, 2820–2838. [CrossRef]

59. Dobler, D.; Huck, T.; Maes, C.; Grima, N.; Blanke, B.; Martinez, E.; Ardhuin, F. Large impact of Stokes drift on the fate of surface floating debris in the South Indian Basin. *Mar. Pollut. Bull.* **2019**, *148*, 202–209. [CrossRef]
60. Morales-Márquez, V.; Hernández-Carrasco, I.; Fox-Kemper, B.; Orfila, A. Ageostrophic contribution by the wind and waves induced flow to the lateral stirring in the Mediterranean Sea. *J. Geophys. Res. Oceans* **2023**, *128*, e2022JC019135. [CrossRef]